LAWRENCE
LIVERMORE
NATIONAL
LABORATORY

UCRL-JRNL-226711

The Application of Global Kinetic Models to HMX Beta-Delta Transition and Cookoff Processes

A. P. Wemhoff, A. K. Burnham, A. L. Nichols III

December 11, 2006

Journal of Physical Chemistry B

The Application of Global Kinetic Models to HMX Beta-Delta Transition and Cookoff Processes

Aaron P. Wemhoff, Alan K. Burnham, Albert L. Nichols III*

Lawrence Livermore National Laboratory, P. O. Box 808, L-227, Livermore, CA, 94551-9900

AUTHOR EMAIL ADDRESS: wemhoff2@llnl.gov

RECEIVED DATE:

TITLE RUNNING HEAD: Application of Global Kinetic Models to HMX

The reduction of the number of reactions in kinetic models for both the HMX beta-delta phase transition and thermal cookoff provides an attractive alternative to traditional multi-stage kinetic models due to reduced calibration effort requirements. In this study, we use the LLNL code ALE3D to provide calibrated kinetic parameters for a two-reaction bidirectional beta-delta HMX phase transition model based on Sandia Instrumented Thermal Ignition (SITI) and Scaled Thermal Explosion (STEX) temperature history curves, and a Prout-Tompkins cookoff model based on One-Dimensional Time to Explosion (ODTX) data. Results show that the two-reaction bidirectional beta-delta transition model presented here agrees as well with STEX and SITI temperature history curves as a reversible four-reaction Arrhenius model, yet requires an order of magnitude less computational effort. In addition, a single-reaction Prout-Tompkins model calibrated to ODTX data provides better agreement with ODTX data than a traditional multi-step Arrhenius model, and can contain up to 90% less chemistry-limited time steps for low-temperature ODTX simulations. Manual calibration methods for the Prout-Tompkins kinetics provide much better agreement with ODTX experimental data than parameters derived from

Differential Scanning Calorimetry (DSC) measurements at atmospheric pressure. The predicted surface temperature at explosion for STEX cookoff simulations is a weak function of the cookoff model used, and a reduction of up to 15% of chemistry-limited time steps can be achieved by neglecting the beta-delta transition for this type of simulation. Finally, the inclusion of the beta-delta transition model in the overall kinetics model can affect the predicted time to explosion by 1% for the traditional multi-step Arrhenius approach, while up to 11% using a Prout-Tompkins cookoff model.

KEYWORDS: explosive, Prout-Tompkins, kinetic models, HMX

1. Introduction

The proper characterization of explosives is vital for proper implementation in military and civilian uses, as well as to ensure safe handling and maintenance. One such explosive, HMX (octahydro-1,3,5,7-tetranitro-1,3,5,7-tetrazocine) has been well-studied in recent years because of its popularity in military applications. The chemical kinetics of this explosive and its related mixtures has been examined via both cookoff experiments and computer simulations.

The One Dimensional Time to eXplosion (ODTX),[1, 2] Scaled Thermal EXplosion (STEX),[3] and Sandia Instrumented Thermal Ignition (SITI)[4] experiments are three well-established methods for characterization of the thermal cookoff properties of explosives. In an ODTX apparatus, the explosive is first pressed into a 1/2”-diameter sphere, and then the explosive is heated isothermally until ignition. In a STEX experiment, the outer surface of a 2”-diameter × 8" long cylinder is heated at a constant temperature ramp rate, typically 1°C/hr, until an explosion occurs. The SITI experiment uses a 1" long × 1" diameter cylinder with an external ramp from room temperature to a maximum temperature, and then held at this maximum temperature thereafter; this ramp rate is based on a desired ramp time of 10-20 minutes. In the ODTX apparatus, two large anvils constrain the external boundary to high pressures, while the STEX and SITI experiments, although sealed by steel casings, allow for some expansion at high pressures. The explosive is initially at room temperature for all three experimental methods.

Temperature measurements of the STEX experiment have also been used to determine characteristics of the endothermic HMX beta-delta phase transition.[3,5] The SITI experiment has been used to characterize the beta-delta transition[4] and for modification of reaction parameters using an inverse heat transfer analysis.[6]

Numerous computer simulations have modeled these cookoff experiments. In many cases, the simulated results have been compared directly to the aforementioned experiments. ODTX time-to-explosion data has been used extensively for comparison to simulated data as a means for testing cookoff kinetic models.[7-9] The vast majority of these models contain two to four sequential first-order, second-order, and autocatalytic Arrhenius reactions to describe each phase transition and lumped chemical decomposition reaction during the cookoff process. Tarver and Tran[7] used this conventional approach to provide good agreement with ODTX and STEX results for a variety of conditions. Yoh *et al*. successfully developed a four-step model for STEX simulations of HMX-based LX-04 and LX-10.[9] In addition, the beta-delta transition model of Henson *et al*.[10] provides an improved prediction of the phase transition half time.

Even though these models are very simplified compared to the real chemical reaction network,[11-15] parameter calibration can be very time consuming, since multiple Arrhenius parameters must be determined. Furthermore, the derived parameters are not necessarily unique because they are often under-constrained, and any error in thermal transport properties can absorbed in the chemical kinetic rate parameters. Therefore, this study examines the potential of consolidating the cookoff process of HMX into two specialized reaction models: one to describe the beta-delta phase transition, and one to characterize the thermal cookoff. In this manner, one can examine the advantage of the easier calibration of a reduced-reaction model versus possible additional flexibility and detail by modeling each sequential phase-transition or chemical-reaction step during a thermal cookoff process. In addition, the use of reduced-reaction models on required computational effort for subsequent applications is examined.

All simulations described in this study use the LLNL code ALE3D, whose chemistry calculation methods are described elsewhere.[16-18] Yoh *et al.* has successfully used this code to model ODTX times and STEX violence for RDX-based explosives.[19]

2. Chemical Kinetic Models

Two types of reactions were analyzed in this study: the beta-delta transition and thermal cookoff.

A. Beta-Delta Transition. Although the beta-delta phase transition of HMX has been studied extensively, the first paper to present a model that satisfies both thermodynamic and kinetic criteria was presented by Henson *et al.*[10] for HMX-based PBX-9501. It includes forward and reverse first-order Arrhenius reactions for nucleation and forward and reverse second-order Arrhenius reactions for growth. This combination, along with appropriate equations of state for the beta and delta phases, allows for the modeling of a first-order phase transition. Although these reactions also include pressure dependencies, the pressure dependencies are neglected for the systems modeled here. The reactions sequence is as follows:

$$\begin{aligned} &\beta \xrightarrow{r_{h1}} \delta \\ &\delta \xrightarrow{r_{h-1}} \beta \\ &\beta + \delta \xrightarrow{r_{h2}} 2\delta \\ &\beta + \delta \xrightarrow{r_{h-2}} 2\beta \end{aligned} \qquad (1)$$

where the kinetic parameters used are

$$\begin{aligned} &\ln A_{h1} = 47.12 \\ &\ln A_{h-1} = 44.39 \\ &\ln A_{h2} = 20.78 \\ &\ln A_{h-2} = 18.04 \\ &E_{h1}/R = 24{,}981\,\mathrm{K} \\ &E_{h-1}/R = 23{,}802\,\mathrm{K} \\ &E_{h2}/R = 9{,}586\,\mathrm{K} \\ &E_{h-2}/R = 8{,}407\,\mathrm{K} \end{aligned} \qquad (2)$$

where A is the frequency factor in s^{-1}, E is the activation energy in J/mol, and R is the ideal gas constant.

While ALE3D can use the forward and reverse reactions explicitly, a potentially more efficient method is to use the bidirectional reaction formalism that also captures the autocatalytic nature of eq 1 to some extent. The beta-delta phase transition is then given by sequential first-order and second-order bidirectional reactions:

$$\begin{aligned} \beta &\xleftrightarrow{r_{b1}} \delta \\ \beta + \delta &\xleftrightarrow{r_{b2}} 2\delta \end{aligned} \qquad (3)$$

for which,

$$\frac{dx}{dt} = -xk \sinh\left(\Lambda_e^* - \frac{E_e^*}{RT}\right) \qquad (4)$$

where x is the fraction remaining of β-HMX, T is temperature, and the values of Λ_e^* and E_e^* set the equilibrium temperature. The parameter k in eq 4 is

$$k(T) = A \exp\left(-\frac{E}{RT}\right) \qquad (5)$$

This above reaction form is similar to the thermodynamically constrained kinetic model used by Burnham[20], which has its roots in early work by Bradley[21],

$$\frac{dx}{dt} = -xk\left(1 - 1/K_{eq}\right) \qquad (6)$$

where K_{eq} is the equilibrium constant,

$$K_{eq} = \exp\left(-\frac{\Delta G}{RT_{eq}}\right) = K_o \exp\left(-\frac{E_e^*}{RT_{eq}}\right) \qquad (7)$$

where ΔG is the free energy change for the transition, K_o is exponential of the entropy change, E_e^* is the enthalpy change, and T_{eq} is the equilibrium temperature. A similar temperature dependence of eqs 4 and 6 may be found by setting both reactions to zero at the equilibrium temperature:

$$\sinh\left(\Lambda_e^* - \frac{E_e^*}{RT_{eq}}\right) \approx 1 - \frac{1}{K_{eq}} = 1 - \frac{1}{K_o \exp\left(-\frac{E_e^*}{RT_{eq}}\right)} \qquad (8)$$

The two functional relations may then be compared using

$$\Lambda_e^* = \frac{E_e^*}{RT_{eq}} = \ln K_o \qquad (9)$$
$$E_e^* = \Lambda_e^* RT_{eq}$$

for known values of T_{eq} and E_e^*.

B. Thermal Cookoff. The cookoff reactions involve the direct transition of β-HMX (or δ-HMX if applicable to a particular overall kinetic model) to gaseous products,

$$\beta \xrightarrow{r_{p1}} prod$$
$$\left(\delta \xrightarrow{r_{p2}} prod\right) \qquad (10)$$

A simple, universal, and functionally accurate kinetic model of the thermal decomposition of HMX is considered here, which would allow for feasible calibration. Henson *et al.* developed a global Arrhenius model based on the plotting of explosion time-temperature data.[22] In addition, Erikson has explored the ability of a variety of global kinetic models to match ODTX data for HMX.[23] He was most successful with four models: an isoconversional model, a linear branching nucleation reaction, an instantaneous nucleation-time dependent growth model, and a cubic autocatalytic model. The simplest of these is the linear chain-branching nucleation model,

$$\frac{dx}{dt} = -k(1 - x) \qquad (11)$$

where x is the fraction remaining of β-HMX (or δ-HMX). This reaction model states that the rate of reaction is related to the amount of product formed, which would be true if the reaction products attack the unreacted material at a rate faster than it decomposes by itself.

An issue with this model is that the initial reaction rate is zero when $x = 1$, so the reaction never

starts unless some initial amount of product has already been formed. There are a couple ways of incorporating this initial condition, but we here choose the method related to the extended Prout-Tompkins model of Burnham,[24] in which

$$\frac{dx}{dt} = -kx^n(1-qx)^m \qquad (12)$$

where eq 11 is formed when n is zero, m is one, and q is an initiation parameter close to one. Equation (12) is actually an approximation to the full autocatalytic equation

$$\frac{dx}{dt} = -k_1 x^{n_1} - k_2 x^{n_2}(1-x)^m. \qquad (13)$$

For $n_1 = n_2 = n$,

$$\frac{dx}{dt} = -k_2 x^n[(1-x)^m + z] \qquad (14)$$

where $z = k_1/k_2 = ((1\text{-}q)/q)^m \approx 1\text{-}q$ for q and $m \sim 1$. In other words, $1\text{-}q$ is the ratio of rate constants for initiation (k_1) and propagation (k_2) and can be considered constant if the activation energies are similar and $k_2 >> k_1$.

In order to correctly apply either of the reactions in eq 10, one must observe that the reaction initiation is dependent upon the total amount of solid HMX available, not just the amount of a particular solid phase. Therefore, the correct application of the Prout-Tompkins model is

$$\frac{dx}{dt} = -kx^n(1-qx_s)^m \qquad (15)$$

where x_s is the total mass fraction of the solid,

$$x_s = x_\beta + x_\delta \qquad (16)$$

Modeling the cookoff using x_β or x_δ for initiation instead of x_s results in dramatically premature predictions of ODTX explosion times for a window of temperature values where both β-HMX and δ-HMX provide significant contributions to the formation of product gases.[25] This phenomenon is expected since the value in the parentheses in eq 15 is always higher when x_S is replaced with x, although this difference is only noticeable when both values of x are approximately equal, or $x \sim x_S/2$.

Therefore, it is important to use the form of eq 15 for modeling the decomposition when including a beta-delta transition in the overall kinetic model.

Note that the parameter q in eq 14 is very close to one, and may therefore be expressed in terms of a parameter p for clarity,

$$p = -\log_{10}(1-q) \qquad (17)$$

This expression contains the characteristic that the value of p is equivalent to the number of nines in q after the decimal point when p is an integer. For example, if $q = 0.999$, then $p = 3.0$.

Numerous multi-step cookoff models are available for HMX processes, such as those developed by Tarver *et al.*,[26] McGuire and Tarver,[27] Sandusky et al.,[28] Hobbs,[29] and Tarver and Tran.[7] We chose the Tarver-Tran model for comparison with the models calibrated in this study because of its good agreement with ODTX and STEX data. The Tarver-Tran kinetic model for coarse HMX contains a series of four sequential Arrhenius reactions, and includes both solid and gaseous intermediate phases (denoted s_i and g_i here). The reaction sequence follows

$$\begin{aligned} &\beta \xrightarrow{r_{t1}} \delta \\ &\delta \xrightarrow{r_{t2}} s_i \\ &s_i \xrightarrow{r_{t3}} g_i \\ &g_i + g_i \xrightarrow{r_{t4}} prod \end{aligned} \qquad (18)$$

and the kinetic parameters are

$$\begin{aligned} &\ln A_{t1} = 48.13 \\ &\ln A_{t2} = 48.70 \\ &\ln A_{t3} = 37.80 \\ &\ln A_{t4} = 28.10 \\ &E_{t1}/R = 24{,}394\,\mathrm{K} \\ &E_{t2}/R = 26{,}522\,\mathrm{K} \\ &E_{t3}/R = 22{,}295\,\mathrm{K} \\ &E_{t4}/R = 17{,}162\,\mathrm{K} \\ &n_{t1} = n_{t2} = n_{t3} = 1 \\ &n_{t4} = 2 \end{aligned} \qquad (19)$$

Tarver and Tran[7] also provide parameters for fine HMX and HMX-based explosives including LX-04, LX-10, and PBX-9501. The difference between LX-04, LX-10, and PBX-9501 is due to the amount and type of secondary material (5% inert Viton binder for LX-10, 15% inert Viton binder for LX-04, and 2.5% binder with 2.5% energetic plasticizer for PBX-9501) as well as the HMX particle size (coarse for LX-10 and PBX-9501, fine for LX-04). Cookoff data are sensitive to the type of explosive used,[7] but a variety of HMX-based explosives provide similar beta-delta transition endotherms in the STEX experiments.[3] Therefore, in this study we provide calibrated kinetic models for coarse HMX, which may be compared to STEX and SITI beta-delta transition endotherms for PBX-9501, and ODTX cookoff results for coarse HMX. We also compare simulated coarse HMX STEX cookoff temperatures with experimental results of LX-04, LX-10, and PBX-9501 since coarse HMX experimental data is unavailable. It should be noted that PBX-9501 experiments exhibit a lower STEX cookoff temperature than either LX-04 or LX-10, which is most likely due to the presence of the energetic plasticizer.

Eight kinetic models, shown in Table 1, were examined in this study to determine the minimal number of reactions required to obtain a reasonable cookoff model for coarse HMX. All models are categorized based on the number of reactions, the kinetic model for beta-delta transition (or lack thereof), and the calibration method for the Prout-Tompkins kinetics (details on the Prout-Tompkins calibration kinetics are provided in the next section). In this study, simulations were performed using each of these kinetic models for comparison of simulated and experimental results, and also to provide insight into computational cost. Models 1 through 6 used energy of formation values of +0.033 J/kg and -5.230 J/kg for δ-HMX and products, respectively. Model 7 uses values of +0.042 J/kg, +0.293 J/kg, -0.264 J/kg, and -5.858 J/kg for δ-HMX, solid intermediates, gaseous intermediates, and products, respectively. Model 8 is the same as Model 7, except that the beta-delta transition is removed from the system, causing a direct transition from β-HMX to solid intermediates. The values of the temperature-dependent thermal properties for the various HMX phases for Models 1 through 6 matched those

provided by Wemhoff and Burnham,[25] and Models 7 and 8 matched those by Tarver and Tran.[7] It should be noted that the energies of reaction used are approximate based on combustion to major products, which may not be appropriate for many applications. Furthermore, the parameters developed in this study are pertinent only to the reaction energies and thermal properties used in this study, and these parameters will not be applicable when different reaction energies or thermal properties are used.

Table 1. Kinetic Models Used in this Study

Model Number	Number of Reactions	Beta-Delta Model	Cookoff Model	Prout-Tompkins Calibration Method	Notes
1	1	None	Prout-Tompkins	DSC	No delta phase, only direct β-HMX transition to products
2	1	None	Prout-Tompkins	ODTX	
3	3	Eq. (3)	Prout-Tompkins	DSC	
4	3	Eq. (3)	Prout-Tompkins	ODTX	PT parameters same as Model 2
5	3	Eq. (3)	Prout-Tompkins	ODTX	Include beta-delta transition during iterative calibration
6	6	Eq. (1)	Prout-Tompkins	ODTX	beta-delta phase transition simulated using model by Henson *et al.*;[10] PT parameters same as Model 2
7	4	Eq. (18)	Arrhenius	N/A	Use four-reaction model by Tarver and Tran[7]
8	3	None	Arrhenius	N/A	Use four-reaction model by Tarver and Tran,[7] except no beta-delta

					phase transition

3. Determination of Reaction Parameters

Determination of chemical kinetics parameters can be found in two ways. One means is by measuring the reaction rate in small samples by either mass loss (thermogravimetric analysis, TGA) or heat release (differential scanning calorimetry, DSC).[30] The second method is to adjust the kinetic parameters to match the explosion times and temperature profiles of larger experiments. In this study, we provide calibrated Prout-Tompkins parameters using both approaches: one set of Prout-Tompkins parameters is based on DSC data, and another set of Prout-Tompkins parameters is calibrated using ODTX data. The bidirectional parameters were calibrated using STEX and SITI temperature profiles. All calibrations based on ODTX, STEX, and SITI experimental data used the LLNL code ALE3D to couple thermal conduction with heat generation from chemical reactions.

A. Bidirectional Reaction. The bidirectional kinetic parameters in eq 3 were calibrated to qualitatively match temperature history profiles along the midplane of the cylindrical SITI test apparatus[4] and at the center of the STEX cylinder. The calibrations were based on the SITI and STEX experiments with PBX-9501. In this SITI test, the ramp rate is 7°C/hr, and the maximum temperature is 192°C. The STEX geometry was modeled as an infinitely-long cylinder since the explosive is heated radially, and the cylinder length is much longer than the diameter (8" long versus 2" diameter). Simulations of the STEX geometry featured a simple one-dimensional mesh of 50 elements with axisymmetry, while the SITI setup was modeled using a two-dimensional 50×50 mesh with axisymmetry. In all simulations, mass scaling was used since no grid motion nor pressure effects were considered. Burnham *et al.*[20] developed parameters for the beta-delta phase transition of eq 1 using DSC measurements at atmospheric pressure. However, these values predicted too high of a phase transition temperature compared to the STEX data, so in this study all parameters except the frequency factor A_{b2} were fixed at the DSC-calibrated values, and A_{b2} was then manually iterated until the

simulated temperature contours matched those experimentally determined from the SITI experiment.[4] The resultant values of the kinetic parameters for this model are:

$$\begin{aligned}
&\ln A_{b1} = 78.29 \\
&\ln A_{b1} = 5.99 \\
&E_{b1}/R = 38{,}817\,\mathrm{K} \\
&E_{b2}/R = 3{,}523\,\mathrm{K} \qquad (20) \\
&n = 1 \\
&T_{eq} = 160^{\circ}\mathrm{C} \\
&K_o = 15.3
\end{aligned}$$

It should be noted that calibration based on X-ray diffraction experiments by Zaug[31] yielded a calibrated value of A_{b2} that was an order of magnitude less,[32] but the resultant temperature profiles did not agree well with STEX and SITI data. Possible reasons for this discrepancy may be due to the consistency of explosive used (the X-ray diffraction experiments used powdered HMX, while the STEX and SITI used packed materials containing both HMX and a binder), or the confinement of the explosive. The experimental curves used for calibration are shown in Figure 1, and the resultant simulated curves for the two-reaction bidirectional model of eq 3 are shown in Figure 2. The four-reaction Arrhenius model by Henson *et al*. of eq 1 and the single-reaction Arrhenius model of eq 18 are shown in Figures 3 and 4, respectively. The figures clearly show that the two-reaction bidirectional model and the four-reaction Arrhenius model exhibit good qualitative agreement between the experimental and simulated values, but the single-reaction Arrhenius model does not show the characteristic drop in the interior temperature profiles.

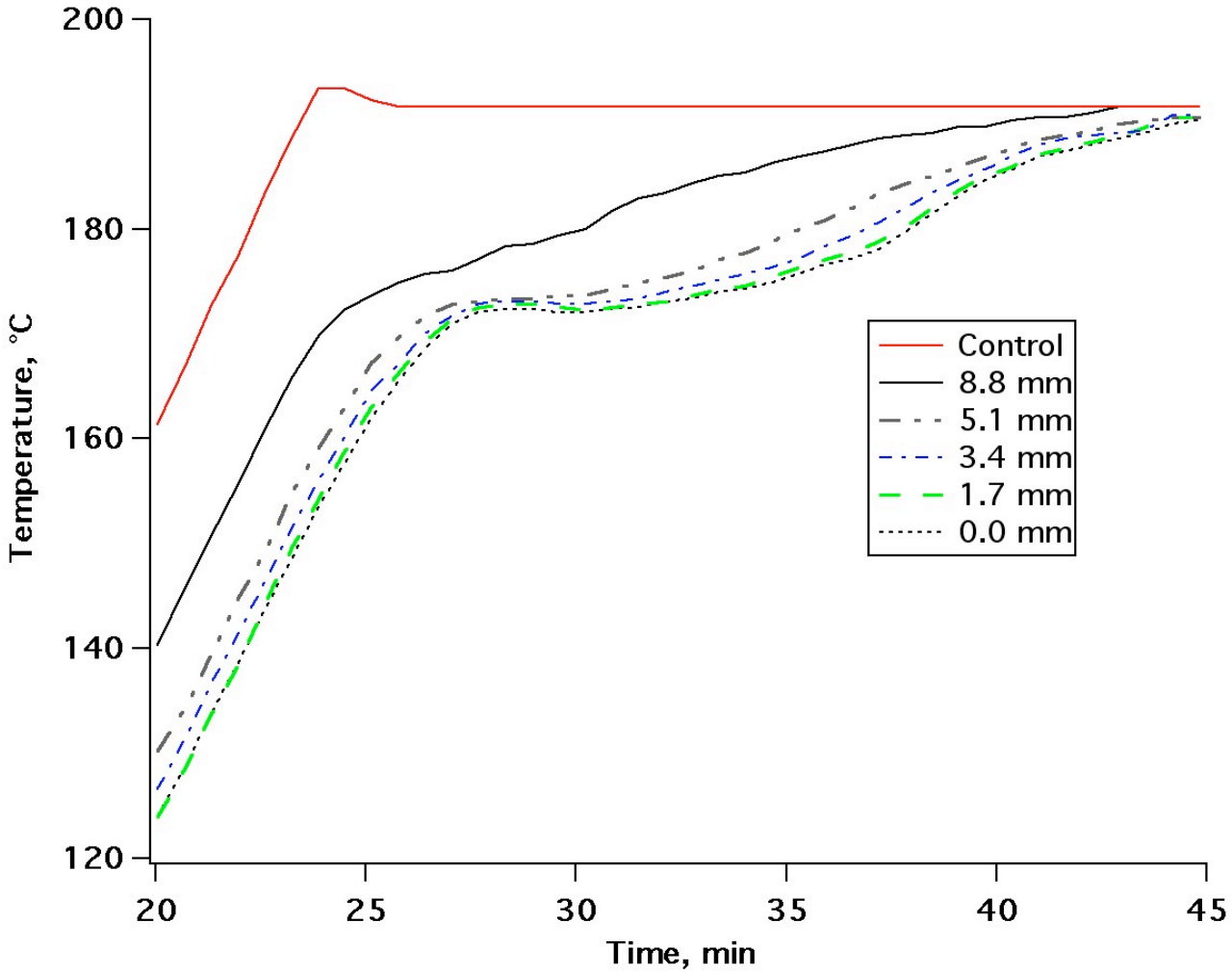
200
180
160
140
120
Temperature, °C
20
25
30
35
40
45
Time, min
Control
8.8 mm
5.1 mm
3.4 mm
1.7 mm
0.0 mm

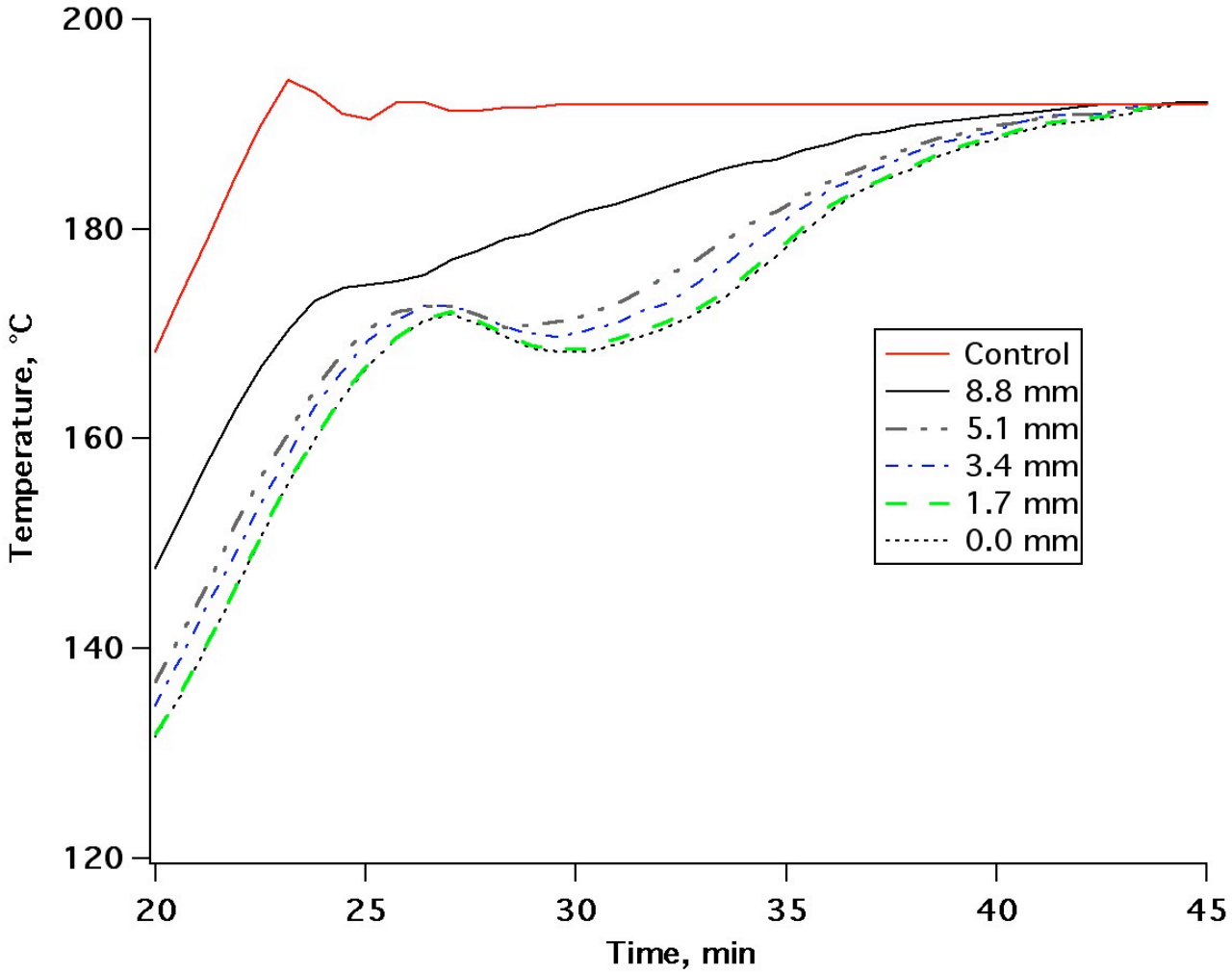

Figure 1. Experimental data by Kaneshige *et al.*[4] for SITI experiments using PBX-9501. Top figure has 9.6% expansion volume, and bottom figure has 13.8% expansion volume (reproduced with author's permission).

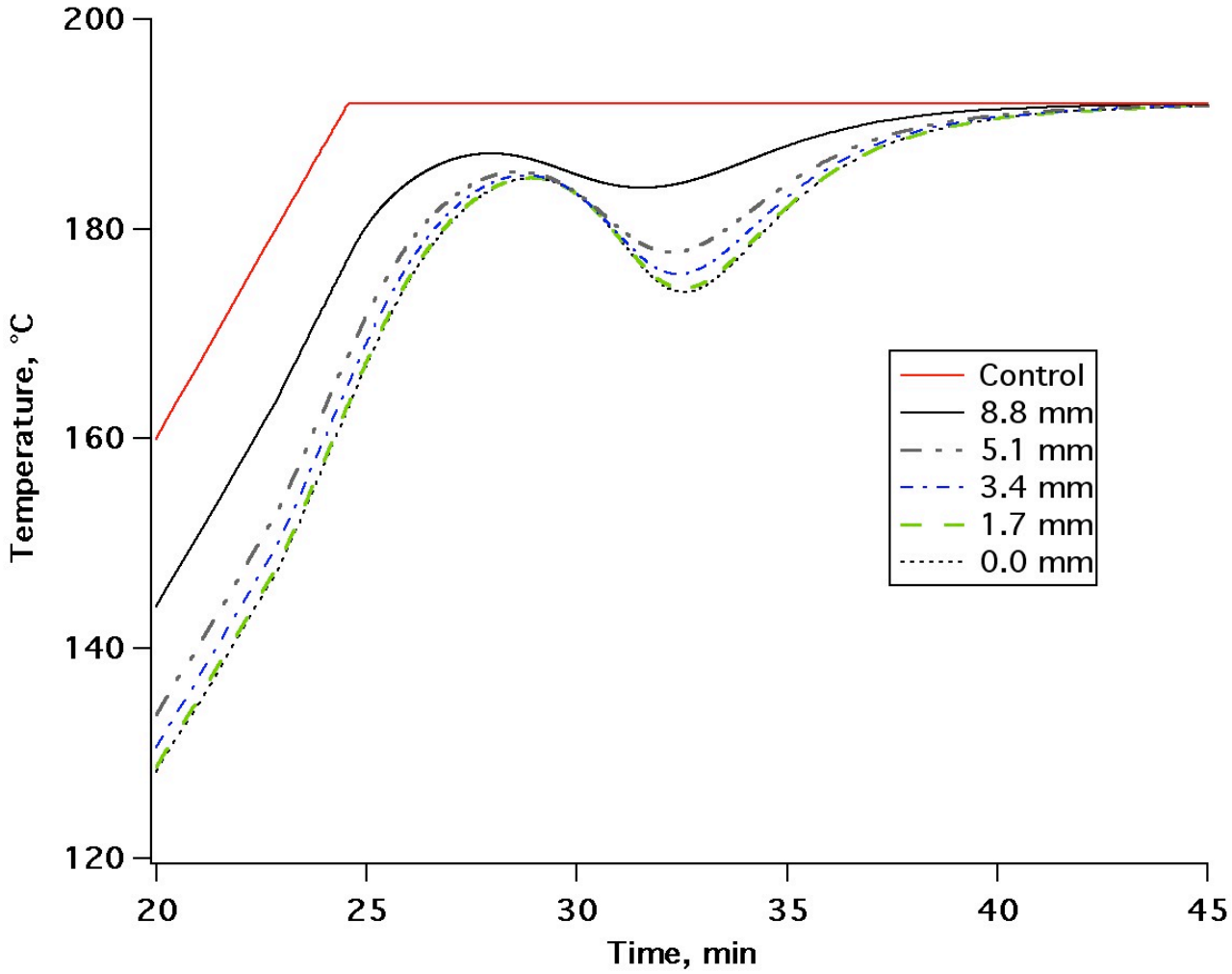

Figure 2. Simulated temperature curves of the coarse HMX SITI apparatus at various diameters along the cylinder midplane using the two-reaction bidirectional beta-delta phase transition model of eq 1.

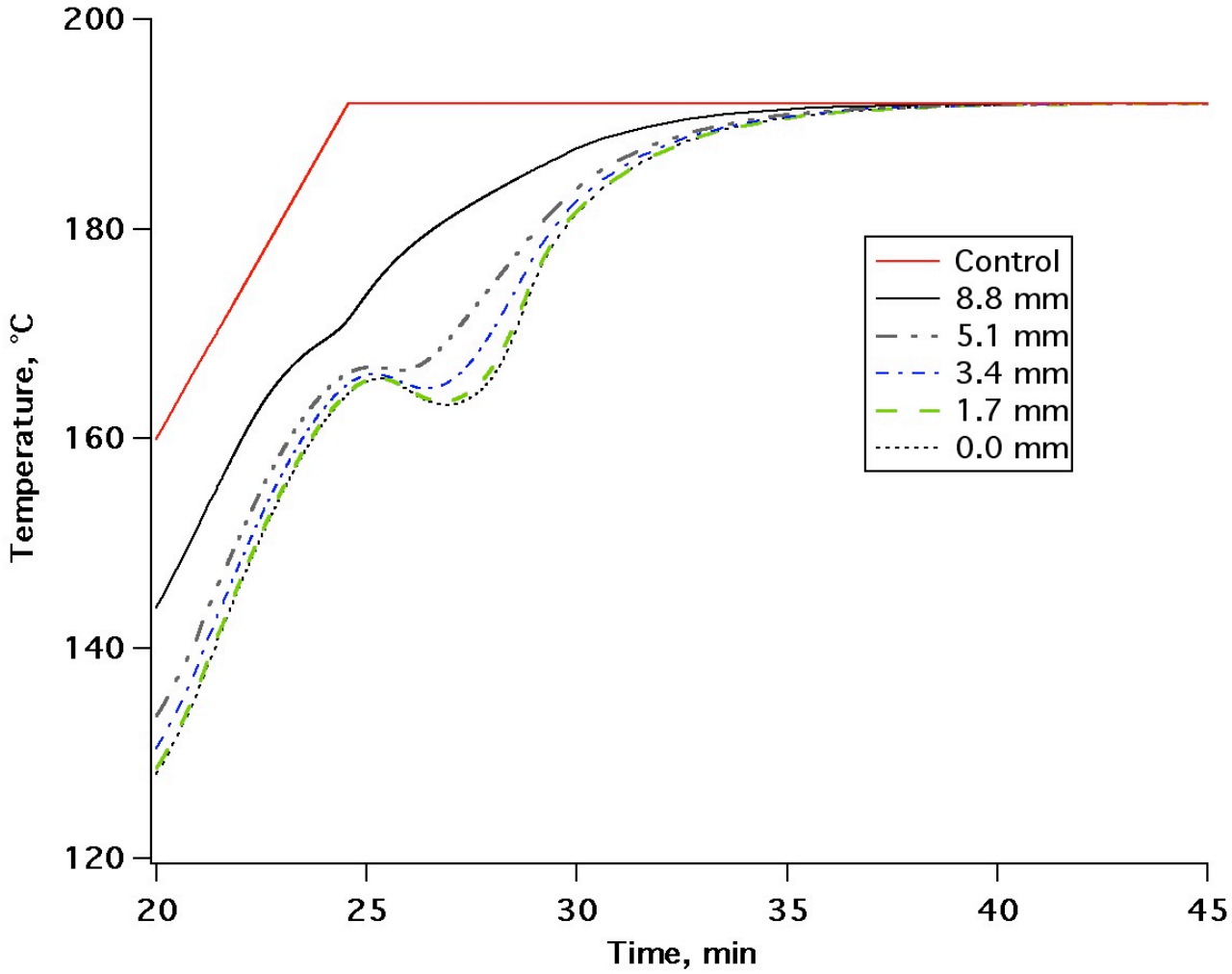

Figure 3. Simulated temperature curves of the coarse HMX SITI apparatus at various diameters along the cylinder midplane using the four-reaction Arrhenius beta-delta phase transition model of Henson *et al.*[10] in eq 18.

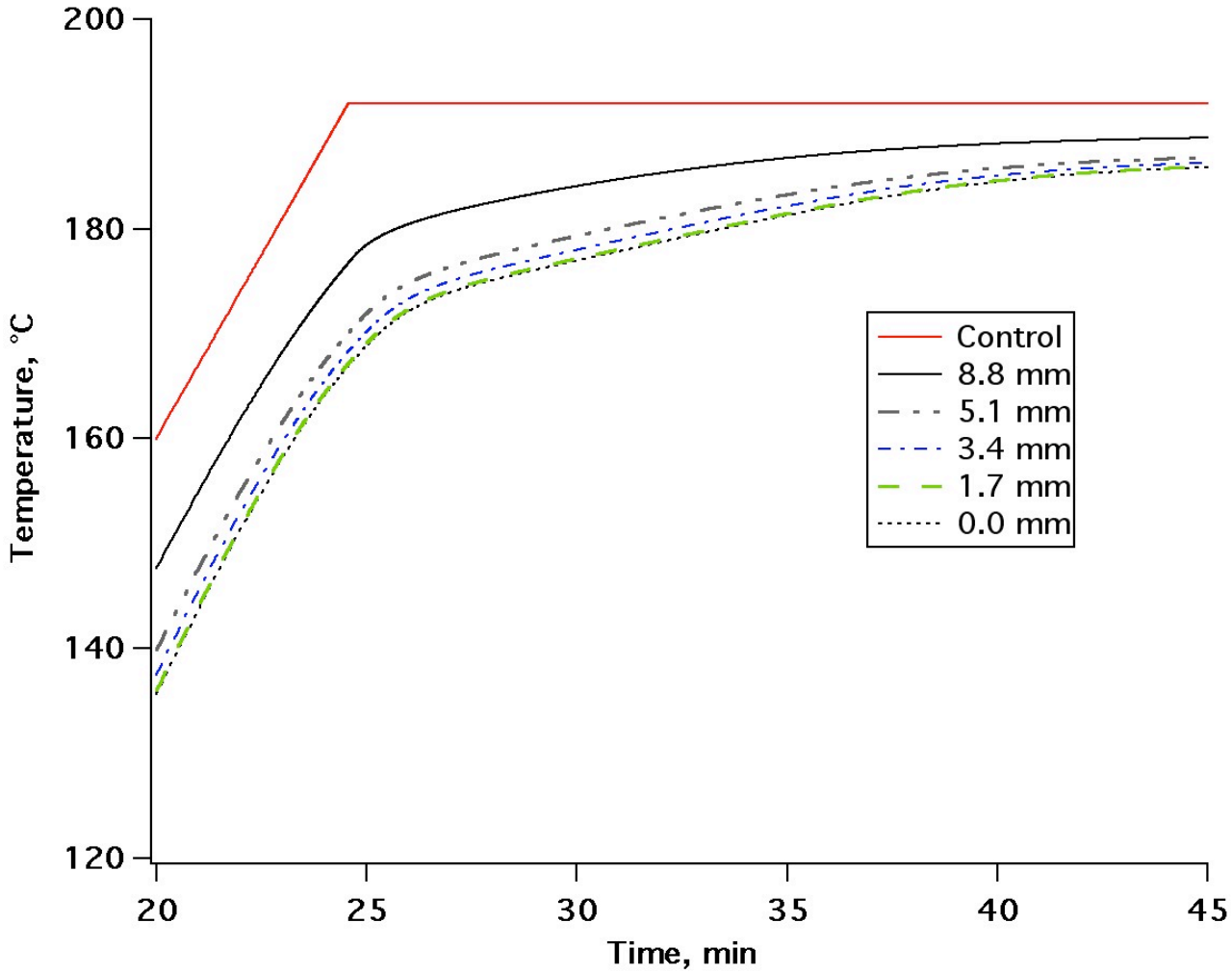

Figure 4. Simulated temperature curves of the coarse HMX SITI apparatus at various diameters along the cylinder midplane using the single-reaction Arrhenius beta-delta phase transition model of Tarver and Tran[7] in eq 8.

Figure 5 provides simulated STEX temperature profiles for comparison with experimental data. The two-reaction bidirectional and four-reaction Arrhenius kinetic models fall within the range of the three transition temperatures exhibited by experiments of PBX-9501, LX-04, and LX-10, although the shapes of the endotherms differ from the experiment because they neglect pressure effects on the phase change temperature. Note that the PBX-9501 demonstrates exothermicity after the transition, which indicates the effect of the energetic binder. The single-reaction Arrhenius model does not indicate a

noticeable temperature drop during the phase transition. This fact suggests that the beta-delta transition aspect of the overall kinetics model in eq 18 may be neglected, and the issue is discussed later in this paper.

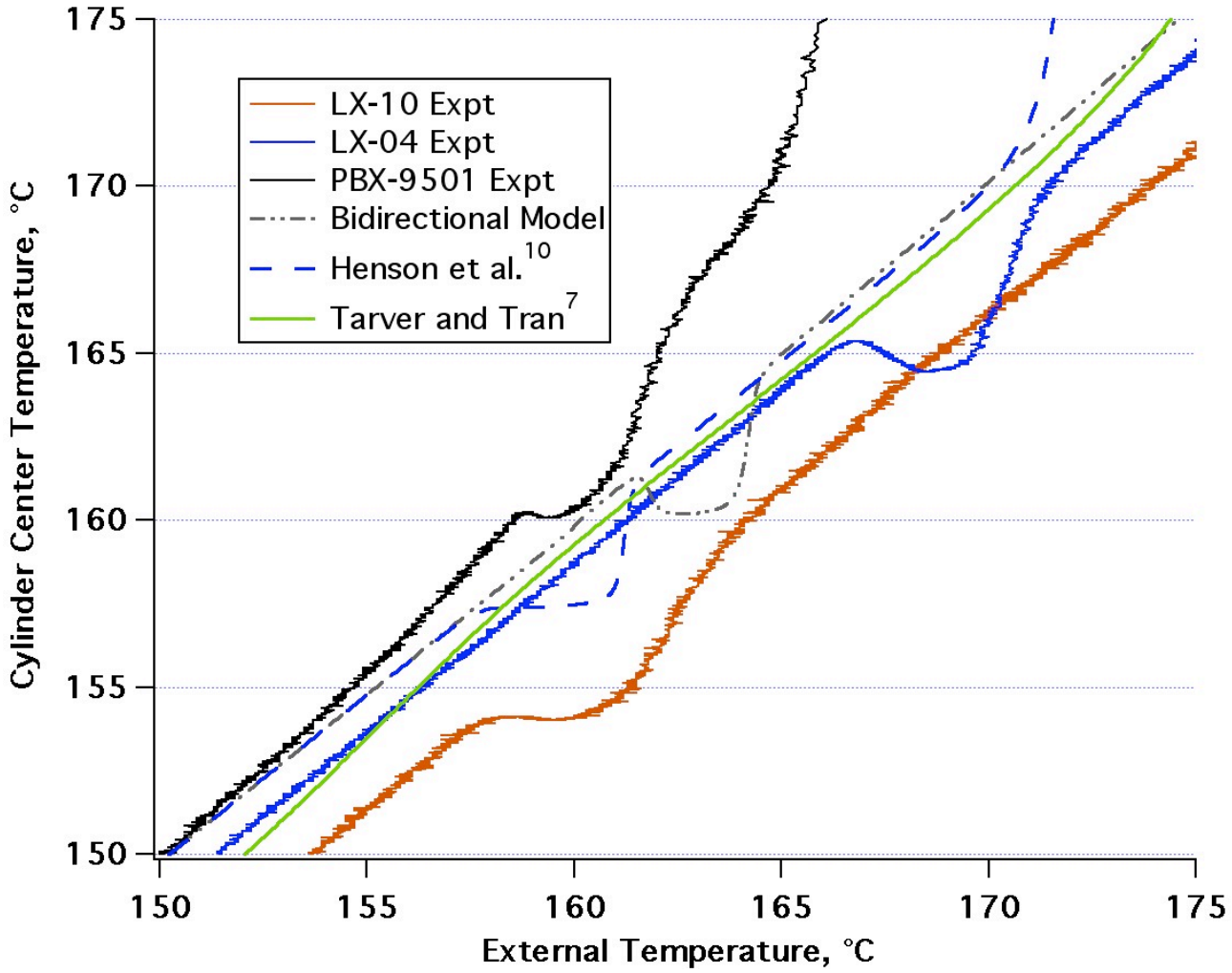

Figure 5. Experimental (PBX-9501, LX-10, and LX-04) and simulated (coarse HMX) temperature history profiles at the center of a cylinder for the STEX setup.

B. Prout-Tompkins Reaction. In the case of the Prout-Tompkins reactions, equivalence of parameters was assumed for the decomposition of both β-HMX and δ-HMX in eq 10. Prout-Tompkins parameters were determined either through DSC results[30] or through a combination of manual iteration and least-squares fitting through known ODTX results. The DSC-based parameters are as follows:

$$\ln A_{p1} = \ln A_{p2} = 31.27$$
$$E_{p1}/R = E_{p2}/R = 19,775\,\mathrm{K}$$
$$n_{p1} = n_{p2} = 0.320 \qquad (21)$$
$$m_{p1} = m_{p2} = 0.635$$
$$p_{p1} = p_{p2} = 2$$

The manual iteration calibration methodology stems from examination of the effect of varying Prout-Tompkins parameters on ODTX explosion times. Therefore, several test runs of an example explosive with generic properties were performed to determine the effect of varying these parameters. All ODTX simulations used a 1×50-element piton mesh with an angle of 4°. In these runs, the parameters E/R and A were maintained at 20,000 K and 1×10^{15} sec^{-1}, respectively, except in a single case where A was adjusted to match the highest temperature data point between curves for $n = 0$, $m = 1$ and $n = 0$, $m = 0$. The two extreme values of p were used in Figures 6a and 6b ($p = 9$ and 2, respectively), where any value of p less than 2 is unphysical per the Prout-Tompkins approximation of eq 14, while any value higher than 9 is read as $q = 1$ in ALE3D, which inhibits the initiation of the reaction. The values of n used were 0.0 and 1.0, while the values of m used were 0.0, 0.5 and 1.0. The "explosion" was deemed to occur when thermal runaway forces the allowable ALE3D time step below a floor of 0.01 microseconds, which roughly corresponds to 5,000 degrees of temperature rise per microsecond in at least one element. These curves suggest the following:

- Increasing the parameter p tends to flatten out the ODTX trend and generally increases the time to explosion (i.e. it shifts the curve upwards).
- Increasing the parameter m also tends to flatten out the curve and shifts it upward in a manner similar to increasing p, although the value of m has a more pronounced effect on the location of the bend in the curve.
- Increasing the parameter n has very little effect on data except near the critical temperature.

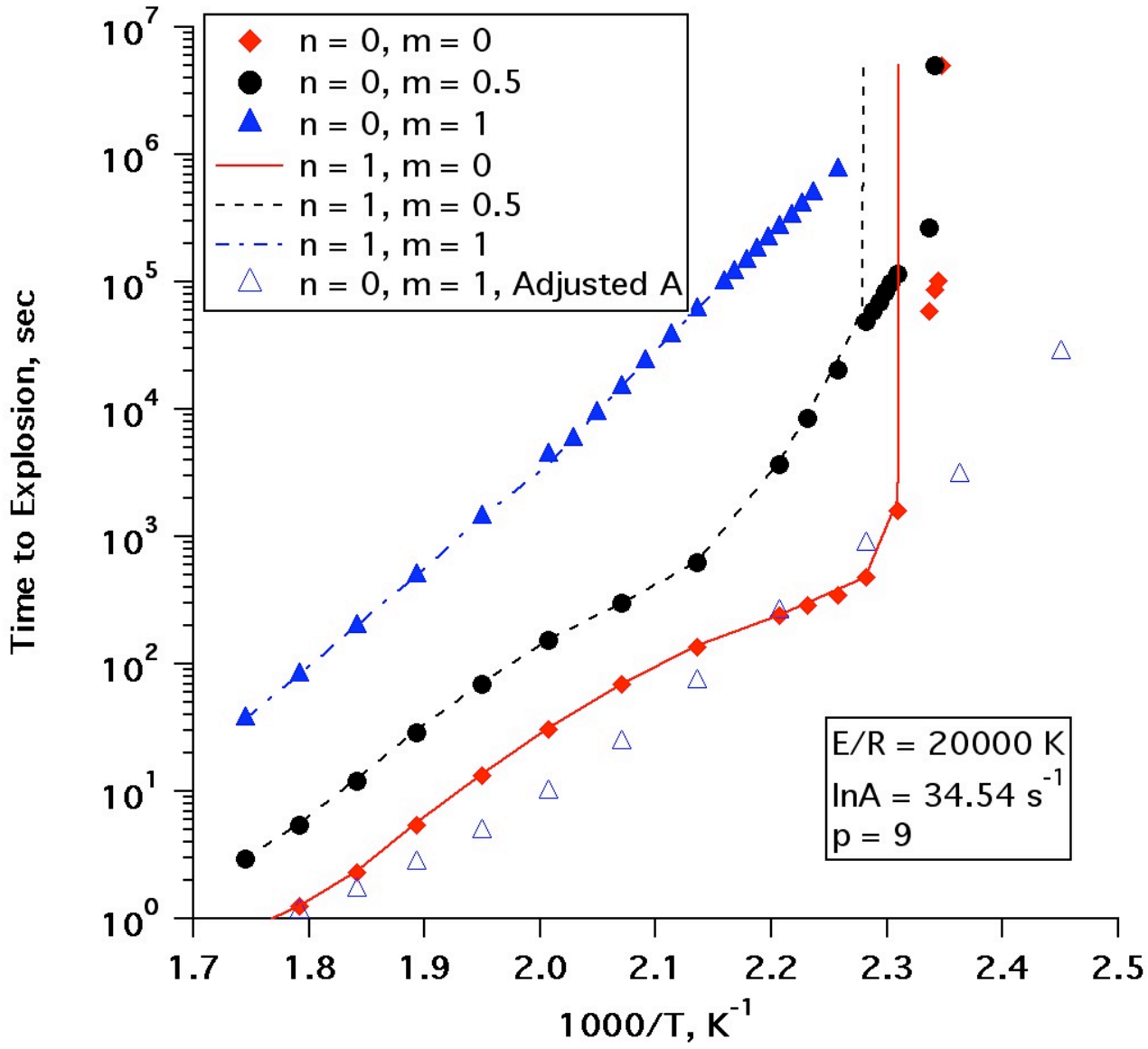

Figure 6a. Simulated ODTX trends of a generic explosive for $p = 9$. The value of adjusted frequency factor for open triangles is $\ln A = 41.49$.

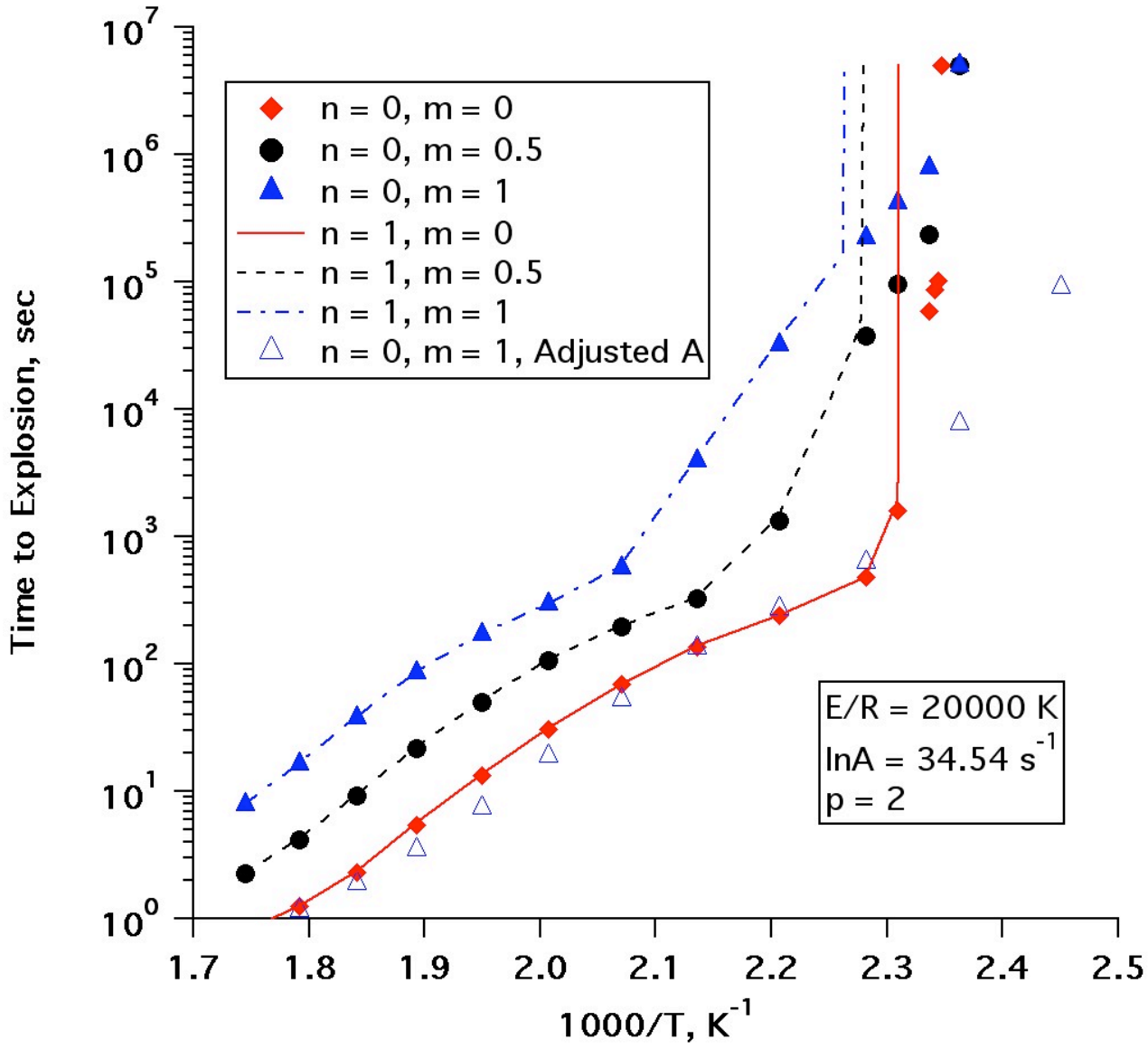

Figure 6b. Simulated ODTX trends of a generic explosive for $p = 2$. The value of adjusted frequency factor for open triangles is $\ln A = 38.58$.

Figures 6a and 6b suggest that a reasonable calibration procedure consists of fixing p based on the observed data: if a bend is present, then set p to a low value (~ 2); if the data appear in a straight line, then set p to a high value (~9). The figures also show that the value of m, A, and E have substantial effects on the magnitude and shape of the curve, while n has an effect only near the critical temperature. Therefore, an iterative approach was used for a rough calibration of Prout-Tompkins parameters based

on the known coarse HMX ODTX times for three temperatures:[33]

1. Estimate a value of *m*.
2. Determine the natural log of the frequency factor *A* at one ODTX temperature T_1. This was done by setting the activation energy to some approximate value (generally E/R ~ 15,000 K), estimating the limiting bounds of ln*A*, and iterating on ln(*A*) using a standard linear interpolation scheme until convergence:

$$\left[\ln A\right]_{new} = \left[\ln A\right]_{min} + \left(\left[\ln A\right]_{max} - \left[\ln A\right]_{min}\right)\left(\frac{t_{goal} - t_{min}}{t_{max} - t_{min}}\right) \qquad (22)$$

where t_{goal} is the experimentally-determined ODTX time, and t_{min} and t_{max} are the times associated with the minimum and maximum values of *A*. It should be noted that function weighting was also used on top of the above interpolation scheme to expedite convergence.[33]

3. Determine the activation energy and frequency factor for a second temperature T_2 using the compensating relationship between *A* and *E*. The relation coupling the two values is

$$k_c = \text{constant} = A\exp\left(-\frac{E}{RT_1}\right) \quad (23)$$

where T_1 is the temperature for the first ODTX data point. The value of k_c is determined using A and E for the first point, and then ln(*A*) was iterated for the second point using eq 22 while the corresponding value of *E* was automatically adjusted using eq 23. The ending value of $k = k_c$ is equivalent for both ODTX temperatures upon convergence.

4. Run a simulation at a third ODTX temperature T_3 and compare to experimental results.
5. Iterate the value of *m* according to an expression for *m* equivalent to eq 10 and go to Step 2 until the value of *m* is determined that allows for convergence at the third temperature.

The manually calibrated kinetic model was then fine-tuned using the LLNL code Global Local Optimizer (GLO),[34] which adjusted the parameters using the method of steepest descents to match data at ten ODTX temperatures. The optimization was based on a calculated figure of merit of

$$FOM = \sum_{i=1}^{10} \left[\ln\left(t_{calc} / t_{goal} \right) \right]_i^2 \qquad (24)$$

where t_{calc} and t_{goal} are the calculated and target times, respectively. The resultant kinetic parameters for the Prout-Tompkins reactions in Models 2, 4, and 6 are

$$\begin{aligned} &\ln A_{p1} = \ln A_{p2} = 34.69 \\ &E_{p1}/R = E_{p2}/R = 18{,}986\,\mathrm{K} \\ &n_{p1} = n_{p2} = 2.72 \times 10^{-6} \\ &m_{p1} = m_{p2} = 1 \\ &p_{p1} = p_{p2} = 9 \end{aligned} \qquad (25)$$

and for Model 5 are

$$\begin{aligned} &A_{p1} = A_{p2} = 34.47 \\ &E_{p1} = E_{p2} = 18{,}877\,\mathrm{K} \\ &n_{p1} = n_{p2} = 0.6688 \\ &m_{p1} = m_{p2} = 1 \\ &p_{p1} = p_{p2} = 9 \end{aligned} \qquad (26)$$

Figures 7a-7c provides comparisons between experimental ODTX results and simulated values using all seven kinetic models, and Table 2 summarizes the average difference between each of the simulated values and their corresponding experimental values. The figures and table clearly show that the models with the DSC-based Prout-Tompkins kinetic parameters do not agree with experimental data as well as those using the iterative calibration procedure. This is due in large part to the existence of the bend in simulated data for the DSC-based models due to $p = 2$, which does not appear in the experimental data trend. Figure 7a also shows that the beta-delta transition only has an effect for a temperature window of 200°C to 240°C, which is primarily due to the fact that the decomposition of β-HMX and δ-HMX are both significant in this range, while the decomposition of δ-HMX dominates for lower temperatures, and β-HMX for higher temperatures. Figure 7b shows that the kinetic model for the beta-delta transition tends to reduce the time to explosion by up to 16% when comparing Models 2, 4, and 6. Models 2 and 5 agree reasonably well with the ODTX data, which is not surprising since they

are the only kinetic models that are directly derived from the same ODTX data to which they are being compared. Finally, Figure 7c demonstrates that neglecting the beta-delta transition in the multi-step model of eq 18 does not significantly affect the overall time to explosion.

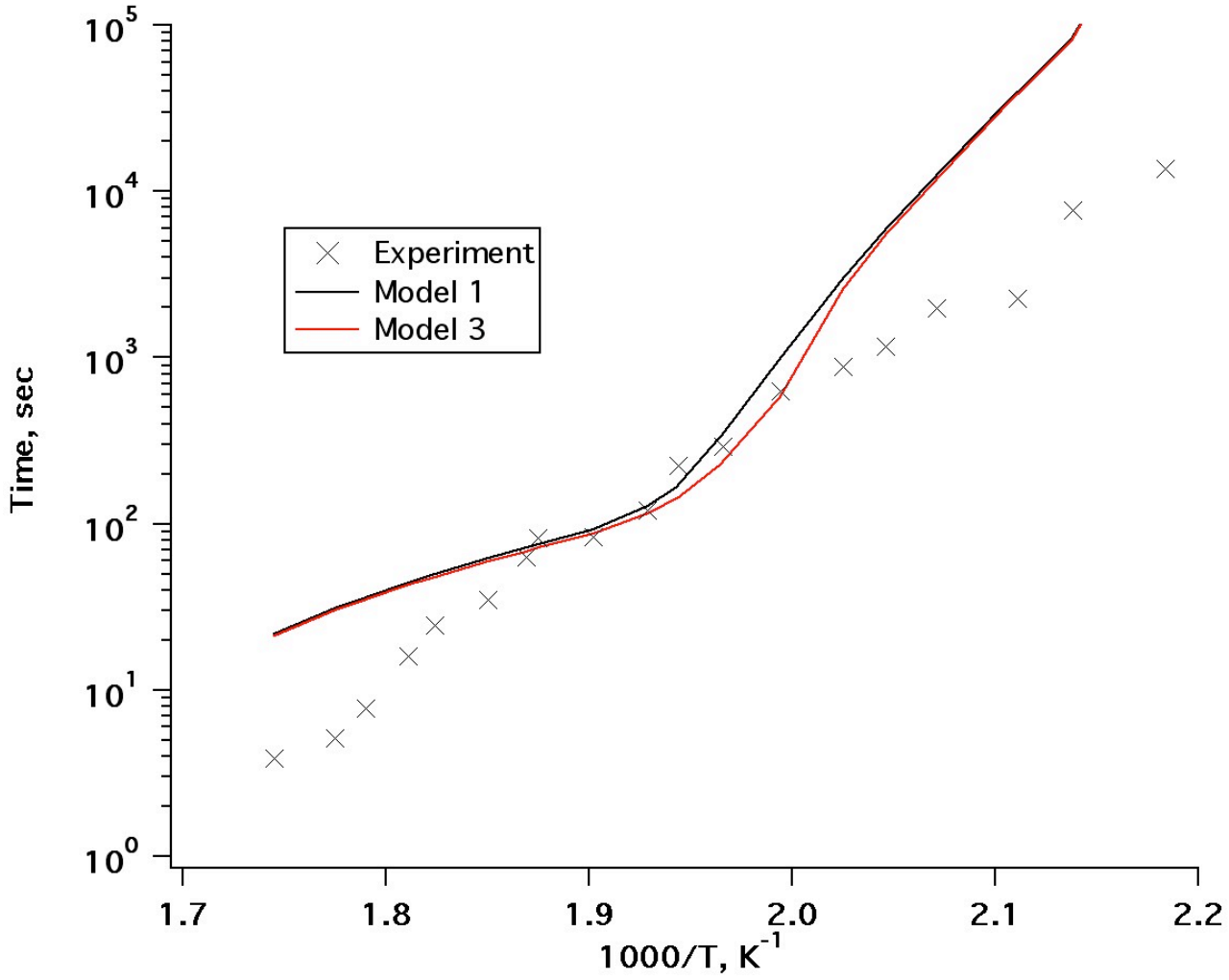

Figure 7a. Comparison of coarse HMX experimental data to simulated ODTX times using DSC-based Prout-Tompkins kinetic parameters. Model 1 omits the beta-delta transition included in Model 3.

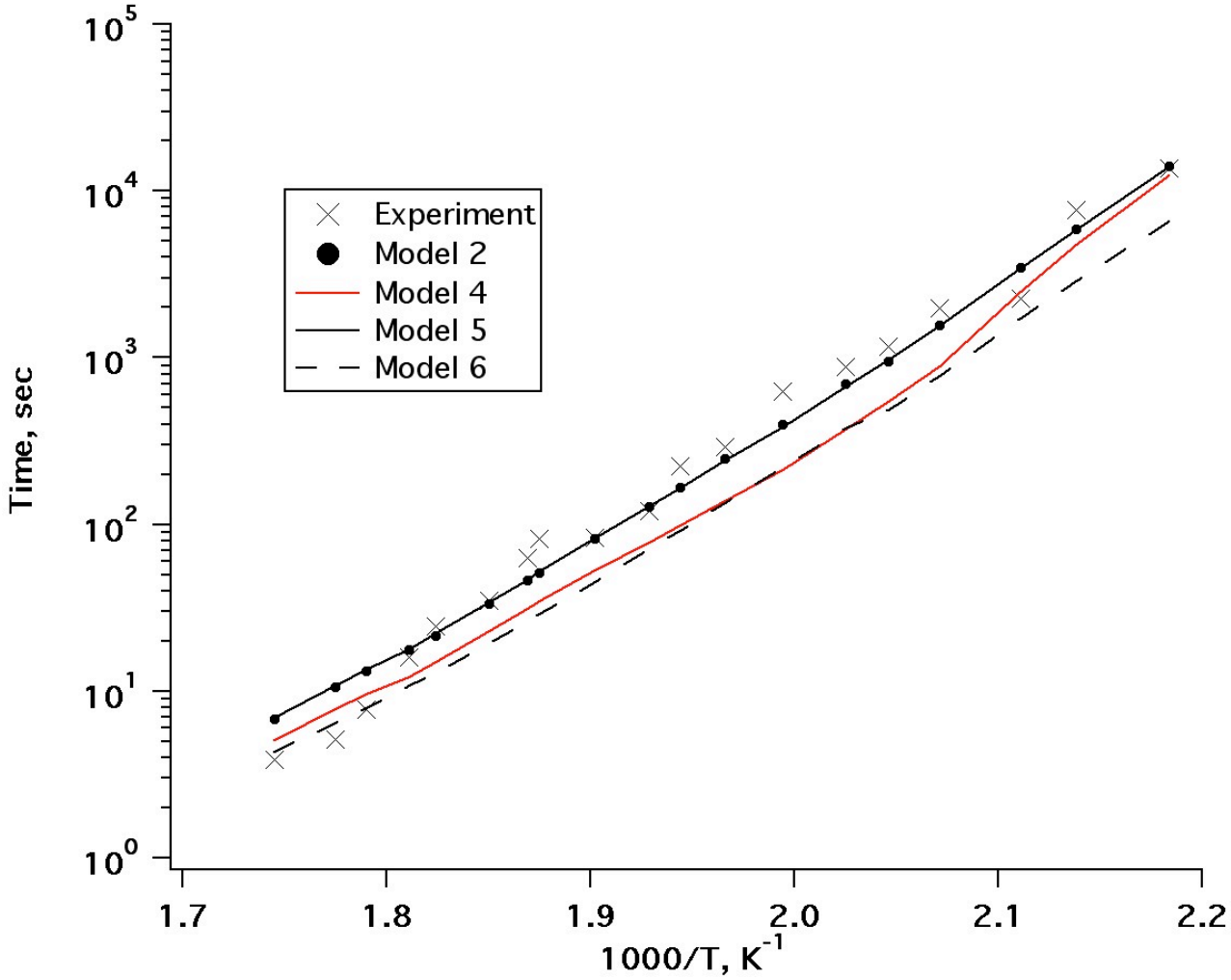

Figure 7b. Comparison of coarse HMX experimental data to simulated ODTX times using manually calibrated Prout-Tompkins kinetic parameters. Models 2, 4, and 6 use the same Prout-Tompkins parameters. Model 2 omits the beta-delta transition, Model 4 uses the two-reaction bidirectional beta-delta model, and Model 6 uses the four-reaction Arrhenius beta-delta model. Model 5 incorporates the two-reaction bidirectional beta-delta transition into the Prout-Tompkins calibration.

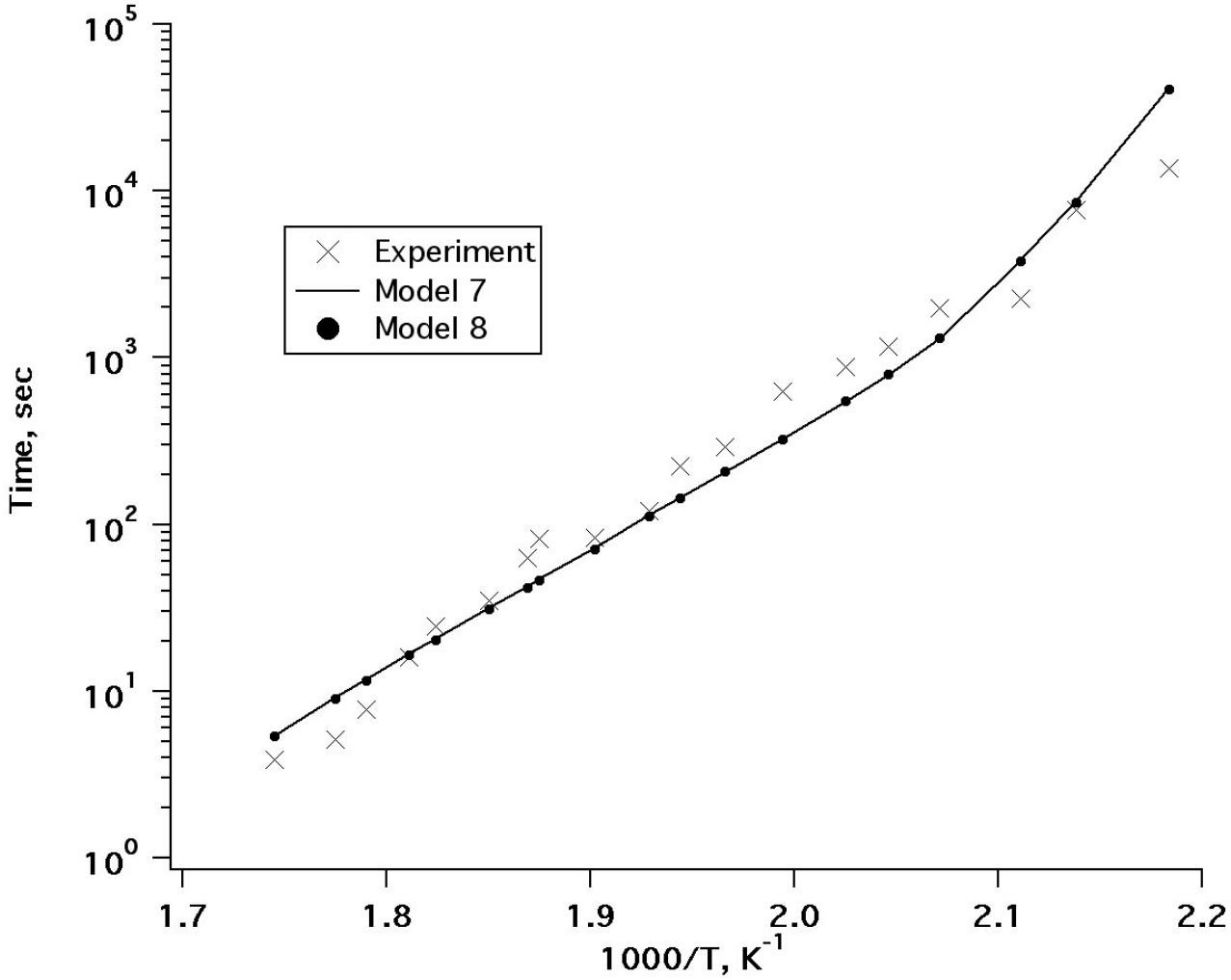

Figure 7c. Comparison of coarse HMX experimental data to simulated ODTX times using models based on that by Tarver and Tran for coarse HMX.[7] Model 8 omits the beta-delta transition in Model 7. The difference between data generated by the two models is negligible.

Table 2. Comparison of Simulated and Experimental HMX ODTX Times to Explosion

Model	Average difference, %
1	567
2	30
3	549
4	41
5	30
6	46

7	42
8	41

STEX cookoff simulations were also run for all eight kinetic models to determine the surface temperature at explosion. The simulation procedure here followed that described earlier in the report for creation of Figure 5. Table 3 below shows that all kinetic models other than Model 6 provide values of surface temperature at explosion that fall within the experimentally determined range. Note that the use of beta-delta transition kinetics does not significantly impact the overall cookoff temperature, which is expected since Figure 5 suggests that the temperature contours recover after the transition is complete. The exception to this is when the four-reaction Arrhenius beta-delta transition model is used, where the kinetics are slightly faster than the other models, and therefore the separation between the endotherm and exotherm is greater.

Table 3. Comparison of Simulated (Coarse HMX) and Experimental (HMX-based Explosives) STEX Surface Temperatures at Explosion for a 1°C/hr Ramp Rate

Model	Surface Temperature at Explosion, deg C
1	188
2	175
3	188
4	175
5	176
6	169
7	178
8	178
Experiment, LX-04[3], Note 1	172-192
Experiment, LX-10[35], Note 2	188

Experiment, PBX-9501[3], Note 3	165-170

Note 1: confinement at 50 MPa gave 172°C, and confinement at 200 MPa gave 187-192°C.

Note 2: confinement at 200 MPa.

Note 3: confinement at 50 MPa gave 170°C, and confinement at 200 MPa gave 165-170°C.

Table 4 provides the calibrated values of all parameters for the various reactions used in this study. Tables 2 and 3 demonstrate that these reactions provide a reasonable approximation to both ODTX and STEX cookoff modeling. The computational advantage of utilizing these kinetics will be explored in the next section.

TABLE 4. Reactions and Values of Parameters Used in this Study

Reaction	Reaction Type	Models where Used	Calibration Method	Parameter values
$\beta \leftrightarrow \delta$	Bidirectional	3, 4, 5	SITI	E/R = 38,817 K ln$A$ = 78.29 Λ_e = 2.728 E_e/R = 1,182 K
$\beta + \delta \leftrightarrow 2\delta$	Bidirectional	3, 4, 5	SITI	E/R = 3,523 K ln$A$ = 5.99 Λ_e = 2.728 E_e/R = 1,182 K
$\beta \rightarrow prod$, $(\delta \rightarrow prod)$	Prout-Tompkins	1, 3	DSC	E/R = 19,775 K ln$A$ = 31.27 m = 0.635 n = 0.320 p = 2.0
$\beta \rightarrow prod$,	Prout-Tompkins	2, 4, 6	Iteration without phase	E/R = 18,986 K

$(\delta \rightarrow prod)$			transition	ln$A$ = 34.69 m = 1.0 n = 2.72×10^{-6} p = 9.0
$\beta \rightarrow prod$, $\delta \rightarrow prod$	Prout-Tompkins	5	Iteration with phase transition	E/R = 18,877 K ln$A$ = 34.47 m = 1.0 n = 0.6688 p = 9.0

4. Computational Effort Comparison

The general computational cost of computing chemical reactions is generally low compared to the overall thermal solution for most practical applications (only about 4% for an ODTX simulation in ALE3D), since chemical reactions in these simulations generally occur in few zones at a time. However, this computational cost could become significant in systems where chemistry occurs in a significant portion of zones at a time. In addition, chemistry calculations generally provide the limiting time step size for a finite element calculation, and minimization of the number of chemistry calls greatly increases computational efficiency. Therefore, the choice of kinetic model can have a significant impact on computational cost, as will be shown in this section.

A. Beta-Delta Transition Models. STEX simulations were run with only the beta-delta phase transition reactions to evaluate the computational cost per call and for the overall simulation. The maximum allowable time step was set at 20 sec for all three calculations, and the simulations were run for a simulated time of 150 hours. The simulations were run in a manner as to provide even computational support for each kinetic model (i.e. each simulation was run sequentially), and 50 sets of simulations were run sequentially to obtain as best an average running time as possible. The

simulations were run on a dedicated processor to eliminate the possibility of other applications using computational resources. Table 5 shows that the four-reaction Arrhenius beta-delta transition model requires an order of magnitude larger time per chemistry call and overall computational time compared to the other two models, while the single-reaction Arrhenius model requires approximately 40% less effort than the two-reaction bidirectional model. However, the single-reaction Arrhenius model cannot properly calculate the transition endotherm nor does it have an effect on time to explosion, so it represents a false savings.

TABLE 5. Computational Effort Required for Beta-Delta Phase Transition in a STEX Simulation

Phase Transition Model	Reference Equation	Computational time per chemistry call (μs/zone/cycle)	Total chemistry computational time (sec)
Single-reaction Arrhenius	eq 18	128	3.5
Two-reaction bidirectional	eq 1	223	6.7
Four-reaction Arrhenius	eq 8	1423	43.8

A further test involved a 250°C ODTX simulation using only the phase transition models in Table 5; cookoff reactions were neglected. The simulation was run for a simulated time of three hours to ensure completion of the phase transition. The single-reaction Arrhenius and two-reaction bidirectional models allowed for rapid convergence of the phase transition kinetics, but the four-reaction Arrhenius model could not converge to within the required radius of convergence. As a result, the single-reaction Arrhenius and two-reaction bidirectional models were completed within 143 and 54 seconds, respectively, while the four-reaction Arrhenius required 1.73 hours of computational time. This

problem did not occur for a 200°C ODTX simulation.

B. Thermal Cookoff Models. The percentage of time steps limited by chemical reaction calculations was also considered for each of the overall kinetic models. In these simulations, the maximum time step used was 10 sec. Table 6 shows that using multi-step Arrhenius models for ODTX simulations (Models 7 and 8) causes nearly all of the time steps to be limited by the chemistry time step, whereas a single-reaction Prout-Tompkins model (Models 1 and 2) is the least inhibitive, especially for low-temperature ODTX simulations. However, the multi-step Arrhenius cookoff model is the least inhibitive for a STEX simulation. Furthermore, Tables 3 and 6 suggest that the inclusion of the two-reaction bidirectional beta-delta transition model does not impact the STEX surface temperature at explosion, yet it slows down the simulation with unnecessary kinetics calculations. However, we cannot state with certainty that absorbing the beta-delta transition into a single-reaction Prout-Tompkins cookoff model (as in Model 2) is always justifiable, for the beta-delta transition kinetics may play a more important role in certain cases, especially near the critical temperature. The difference in computational cost between DSC-calibrated and manually-calibrated Prout-Tompkins kinetics are due to the difference in calculated times to explosion, as shown by Figures 7a and 7b, and thus cannot be evenly compared to each other. Further results from 200°C simulations show that Model 8 took 54% less steps to complete the run compared to Model 7, yet the difference in time to explosion was only 1%. Finally, Model 1 required 18% less steps than Model 3, yet the difference in time to explosion was only 4%.

TABLE 6. Percentage of Chemistry-limited Time Steps in Various Cookoff Simulations

Model	Total Number of Reactions	Percentage of chemistry-limited time steps		
		200°C ODTX simulation	250°C ODTX simulation	STEX simulation
1	1	2	14	4
2	1	12	48	3
3	4	23	14	5

4	4	72	49	6
5	4	68	48	6
6	6	97	99	20
7	4	97	99	1
8	3	88	96	1

5. Discussion and Conclusions

Thermal explosions are caused by runaway exothermic reactions, and the acceleration can be due to chemical, thermal, and pressure effects. Even though importance of chemical acceleration (autocatalysis) was recognized even in the early 20th century[36,37], early assessments of thermal explosions typically used first-order or zero-order reactions kinetics in order to get tractable mathematical solutions for thermal explosion times.[37,38] However, such simplistic chemical kinetic models do not produce the correct relationship between explosion time and reciprocal temperature in ODTX,[1] so Tarver et al.[26] developed the multistep reaction models in combination with numerical integration of thermal transport to avoid the need for unrealistic mathematical simplification to obtain the correct functional form. This approach has been refined over the years, but it is increasingly recognized that the reaction parameters are not uniquely determined.[4,8] Others have obtained more detailed chemical kinetic information with the objective of developing a more rigorous mechanistic model,[11-15] but it does not yet exist despite years of effort. Our approach in this work is to look for the simplest mathematical form that honors the most important aspect of the underlying chemistry: autocatalysis. We have shown that a modest extension of the historic nucleation-growth (sigmoidal) kinetic model of Prout and Tompkins works well for that purpose.

A related chemical kinetic problem occurs in materials such as HMX that have a phase transition prior to thermal ignition. We have shown that the consolidation of a four-reaction Arrhenius beta-delta transition kinetic model into a two-reaction bidirectional model provides similar temperature history curves for SITI and STEX simulations, while reducing the overall computational cost for chemical

reactions by an order of magnitude. Furthermore, the lack of noticeable beta-delta transition endotherms for the SITI and STEX simulations using the one-reaction Arrhenius model suggests that the two-reaction bidirectional model is an efficient, reasonably accurate model for modeling this phase transition. It has also been shown that these kinetics may be neglected for STEX simulations.

Figures 7a-d and Table 3 demonstrate that the ODTX predictions are much more sensitive than STEX predictions to the cookoff kinetics used, which is most likely due to the large duration of the STEX test compared to the ODTX test where the temperature is insufficient to support chemical reactions. Therefore, the direct calibration of Prout-Tompkins parameters from ODTX data provides a good approach to developing a global cookoff model. Furthermore, the simplicity of a global kinetic model allows for the ignoring of the details of the individual kinetics that physically make up the ignition process. Therefore, the Prout-Tompkins model contains an acceptable approximation of the chemical kinetic processes during deflagration for many applications.

The global Prout-Tompkins activation energy of 158 kJ/mol derived here from ODTX is similar to the 149 kJ/mol inferred by Henson et al.[22] from a compilation of ignition times for HMX formulations over very wide time and temperature ranges and in the middle of the energy range for the compilation by Brill et al.[39] It is slightly lower than the 167 kJ/mol calculated for the presumed initiation step of N-N bond homolysis, but that might be expected because global activation energies for chain reactions are a complicated average of initiation, propagation, and termination reactions. Global activation energies for hydrocarbon and polymer pyrolysis reactions are typically ~70% of the initiation energies. For example, cracking of n-hexadecane has an apparent global activation energy of ~250 kJ/mol even though the carbon-carbon bond has a strength of 345 kJ/mol.[40]

Even so, the Prout-Tompkins model is less rigorous than a multi-step Arrhenius model and may have more difficulty extrapolating outside its range of calibration than a well chosen and calibrated multistep model. All large-scale (>1g) experiments modeled here were sealed, and the calibrated parameters from this study are not appropriate for either DSC experiments or vented experiments where

pressure is closer to atmospheric. This issue is particularly important for HMX-based explosives, which have an apparent pressure dependence of ~$P^{0.3}$ due to contributions of autocatalytic and bimolecular gas-phase reactions.[41] Nevertheless, with the range of conditions considered in this paper, the manually-calibrated Prout-Tompkins models provides agreement with ODTX and STEX data that rival that for the multi-step model, and allow for a reduction of nearly 90% chemistry-limiting time steps for low-temperature ODTX simulations.

ACKNOWLEDGMENT

This work was performed under the auspices of the U. S. Department of Energy by the University of California, Lawrence Livermore National Laboratory, under Contract No. W-7405-Eng-48.

REFERENCES

1. Catalano E.; McGuire R.; Lee E.; Wrenn E.; Ornellas D.; Walton J. *6th Symposium (International) on Detonation*, Office of Naval Research ACR-221, Coronado, CA, 214, **1976**.

2. Tran T. D.; Simpson L. R.; Maienschein J.; Tarver C. *32nd International Annual Conference*

of Fraunhofer-Institut fur Chemische Technologie (ICT), DWS Werbeagentur & Verlag, Karlsruhe, Germany, 25, **2001**.

3. Wardell J. F.; Maienschein J. L. *12th International Symposium on Detonation*, Office of Naval Research, San Diego, CA, 384, **2002**.

4. Kaneshige M. J.; Renlund A. M.; Schmitt R. G.; Erikson W. W. *12th International Symposium on Detonation*, Office of Naval Research, San Diego, CA, 821, **2002**.

5. Maienschein J. L.; Wardell J. F.; Reaugh J. E. *JANNAF CS/APS/PSHS Joint Meeting*, Monterey, CA, **2000**.

6. Schmitt R. G.; Erickson W. W.; Kaneshige M. J; Renlund A. M. *JANNAF 39th CS, 27th APS, 21st PSHS, and 3rd MSS Joint Meeting*, Colorado Springs, CO, **2003**.

7. Tarver C. M.; Tran T. D. *Combust. Flame* **2004**, *137*, 50.

8. Hobbs M. L.; Kaneshige M. J. *13th International Detonation Symposium*, Norfolk, VA, Report IDS066, **2006**.

9. Yoh J.; McClelland M. A.; Nichols A. L.; Maienschein J. L; Tarver C. M. *13th International Detonation Symposium*, Norfolk, VA, Report IDS158, **2006**.

10. Henson B. F.; Smilowitz L.; Asay B. W.; Dickson P. M. *J. Chem. Phys.* **2002**, *117*, 3780.

11. Levitas V. I.; Henson B. F.; Smilowitz L. B.; Asay B. W. *J. Phys. Chem B* **2006**, *110*, 10105-10119.

12. Behrens R., Jr. *J. Phys. Chem.* **1990**, 98, 6706.

13. Behrens R., Jr.; Bulusu S. *J. Phys. Chem.* **1991**, 95, 5838.

14. Oxley J. C.; Kooh A. B.; Szekeres R.; Zheng W. *J. Phys. Chem.* **1994**, 98, 7004.

15. Chakraborty D.; Muller R. P.; Dasgupta S.; Goddard W. A. III *J. Phys. Chem.* **2001**, 105, 1302.

16. Nichols A. L.; Westerberg K. W. *Numer. Heat Trans. B* **1993**, *24*, 489.

17. Nichols A. L.; Couch R.; McCallen R. C.; Otero I.; Sharp R. *11th International Detonation Symposium*, Snowmass, CO, **1998**.

18. Nichols A. L.; Anderson A.; Neely R.; Wallin B. *12th International Detonation Symposium*, San Diego, CA, **2002**.

19. Yoh J. J.; McClelland M. A.; Maienschein J. L.; Wardell J. F.; Tarver C. M. *J. Appl. Phys.* **2005**, *97*, 083504.

20. Burnham A. K.; Weese R. K.; Weeks B. L. *J. Phys. Chem. B* **2004**, *108*, 19432.

21. Bradley R. S. *J. Phys. Chem.* **1956**, 60, 1347.

22. Henson B. F.; Smilowitz L.; Asay B. W.; Sandstrom M. M.; Romero J. J. *13th International Detonation Symposium*, Norfolk, VA, Report IDS061, **2006**.

23. Erikson W. W. *13th International Detonation Symposium*, Norfolk, VA, Report IDS035, **2006**.

24. Burnham A. K. *J. Therm. Anal. Cal.* **2000**, *60*, 895.

25. Wemhoff A. P.; Burnham A. K. *Comparison of the LLNL ALE3D and AKTS Thermal Safety Computer Codes for Calculating Times to Explosion in ODTX and STEX Thermal Cookoff Experiments*, Lawrence Livermore National Laboratory, Report UCRL-TR-220687, **2006**.

26. Tarver C. M.; McGuire R. R.; Lee E. L.; Wrenn E. W.; Brein K. R. *Proc. Combust. Inst.* **1978**,

17.

27. McGuire R. R.; Tarver C. M. *7th Symposium (International) on Detonation*, Naval Surface Weapons Center NSWC MP 82-334, Annapolis, MD, 56, **1981**.

28. Sandusky H. W.; Chambers G. P.; Erikson W. W.; Schmitt R. G.; *12th International Detonation Symposium,* San Diego, CA, **2002**.

29. Hobbs M. L. *Thermochimica Acta* **2002**, *384*, 291.

30. Burnham A. K.; Weese R. K.; *Thermal Decomposition Kinetics of HMX*, Lawrence Livermore National Laboratory, Report UCRL-TR-204262 Rev 1, **2004**.

31. Zaug J. M.; Farber D. L.; Saw C. K.; Weeks B. L. *Kinetics of Solid Phase Reactions at High Pressure and Temperature*, Lawrence Livermore National Laboratory, Report UCRL-ID-147389, **2003**.

32. Wemhoff A. P.; Burnham A. K. *Calibration of Parameters in Beta-Delta HMX Phase Transformation Kinetics Using Computer Simulations*, Lawrence Livermore National Laboratory, Report UCRL-TR-218130, **2006**.

33. Wemhoff A. P.; Burnham A. K. *Methods for Calibration of Prout-Tompkins Kinetics Parameters Using EZM Iteration and GLO*, Lawrence Livermore National Laboratory, Report UCRL-TR-225940, 2006.

34. Murphy M. J. *GLO - Global Local Optimizer User's Manual*, Lawrence Livermore National Laboratory, Report UCRL-MA-133858, **1999**.

35. Maienschein J. L.; DeHaven M. R.; Sykora G. B.; Black C. K.; Wardell J. F.; McClelland M. A.; Strand O. T.; Whitworth T. L.; Martinez C. *13th International Detonation Symposium*,

Norfolk, VA, Report IDS097, **2006.**

36. D. A. Frank-Kamenetsky, *"Diffusion and Heat Exchange in Reaction Kinetics"***,** Academy of Sciences of the USSR, Princeton University Press, Princeton, New Jersey, 1955 (Translation).

37. Merzhanov A. G.; Abramov V.G. *Propellants and Explosives* **1981**, 6, 130.

38. Zinn J.; Rogers R. N. *J. Phys. Chem.* **1962**, 66, 2646.

39. Brill T. B.; Gongwer P. E.; Williams G. K. *J. Phys. Chem.* **1994**, 98, 12242.

40. Jackson K. J.; Burnham A. K.; Braun R. L.; Knauss K. G. *Org. Geochem.* **1995**, 23, 941.

41. Burnham A. K.; Weese R. K.; Wardell J. F.; Tran T. D.; Wemhoff A. P.; Koerner J. G.; Maienschein J. L. *13th International Detonation Symposium*, Norfolk, VA, Report IDS018, **2006.**